RSC Advances

PAPER

View Article Online
View Journal | View Issue

Cite this: *RSC Adv.*, 2023, **13**, 9333

Tuning anticancer properties and DNA-binding of Pt(II) complexes *via* alteration of nitrogen softness/basicity of tridentate ligands†

Kamelah S. Al-Rashdi,[ab] Bandar A. Babgi,[*a] Ehab M. M. Ali,[cd] Abdesslem Jedidi,[a] Abdul-Hamid M. Emwas,[e] Bambar Davaasuren,[e] Mariusz Jaremko[f] and Mark G. Humphrey[g]

Nine tridentate Schiff base ligands of the type (N^N^O) were synthesized from reactions of primary amines {2-picolylamine (Py), *N*-phenyl-1,2-diaminobenzene (PhN), and *N*-phenyl-1,2-diaminoethane(EtN)} and salicylaldehyde derivatives {3-ethoxy (OEt), 4-diethylamine (NEt_2) and 4-hydroxy (OH)}. Complexes with the general formula Pt(N^N^O)Cl were synthesized by reacting K_2PtCl_4 with the ligands in DMSO/ethanol mixtures. The ligands and their complexes were characterized by NMR spectroscopy, mass spectrometry and elemental analysis. The DNA-binding behaviours of the platinum(II) complexes were investigated by two techniques, indicating good binding affinities and a two-stage binding process for seven complexes: intercalation followed by switching to a covalent binding mode over time. The other two complexes covalently bond to ct-DNA without intercalation. Theoretical calculations were used to shed light on the electronic and steric factors that lead to the difference in DNA-binding behavior. The reactions of some platinum complexes with guanine were investigated experimentally and theoretically. The binding of the complexes with bovine serum albumin (BSA) indicated a static interaction with higher binding affinities for the ethoxy-containing complexes. The half maximal inhibitory concentration (IC_{50}) values against MCF-7 and HepG2 cell lines suggest that platinum complexes with tridentate ligands of *N*-phenyl-*o*-phenylenediamine or pyridyl with 3-ethoxysalicylimine are good chemotherapeutic candidates. **Pt-Py-OEt** and **Pt-PhN-OEt** have IC_{50} values against MCF-7 of 13.27 and 10.97 μM, respectively, compared to 18.36 μM for cisplatin, while they have IC_{50} values against HepG2 of 6.99 and 10.15 μM, respectively, compared to 19.73 μM for cisplatin. The cell cycle interference behaviour with HepG2 of selected complexes is similar to that of cisplatin, suggesting apoptotic cell death. The current work highlights the impact of the tridentate ligand on the biological properties of platinum complexes.

Received 18th January 2023
Accepted 14th March 2023

DOI: 10.1039/d3ra00395g

rsc.li/rsc-advances

1 Introduction

Cisplatin (Fig. 1) was the first approved alkylating-like chemotherapeutic drug that is known to bind DNA covalently. It is activated for binding by the hydrolysis of its labile chlorido ligands, to produce *cis*-$[Pt(NH_3)_2Cl(H_2O)]^+$.[1] Inside the cell, the aqua ligand is exchanged with N_7-guanine, producing a *cis*-$[Pt(NH_3)_2Cl(DNA)]^+$ adduct.[2] The second chlorido ligand undergoes a similar process to form a cross-linked DNA (either intra-strand or inter-strand).[3] The drug-DNA binding causes conformational changes to DNA, promoting apoptotic cell death.[4,5] Although cisplatin is clinically approved and is used to treat a range of cancer types, it has several drawbacks, including lack of selectivity toward cancer cells, acquired resistance, and severe side effects.[6–10] Many platinum(II) complexes have been developed as possible alternatives, modifying the structure of cisplatin by replacing either the leaving groups (chlorido) and/or the non-leaving groups (ammine) by a range of ligands. These modifications have resulted in a few clinically approved

[a]*Department of Chemistry, Faculty of Science, King Abdulaziz University, P.O. Box 80203, Jeddah 21589, Saudi Arabia. E-mail: bbabgi@kau.edu.sa; Tel: +966 555563702*

[b]*Department of Chemistry, Al-Qunfudah University College, Umm Al-Qura University, Al-Qunfudah 1109, Saudi Arabia*

[c]*Department of Biochemistry, Faculty of Science, King Abdulaziz University, P.O. Box 80203, Jeddah 21589, Saudi Arabia*

[d]*Division of Biochemistry, Department of Chemistry, Faculty of Science, Tanta University, Tanta 31527, Egypt*

[e]*Core Labs, King Abdullah University of Science and Technology (KAUST), Thuwal, 23955-6900, Saudi Arabia*

[f]*Biological and Environmental Science and Engineering (BESE), King Abdullah University of Science and Technology (KAUST), Thuwal, 23955-6900, Saudi Arabia*

[g]*Research School of Chemistry, Australian National University, Canberra, ACT 2601, Australia*

† Electronic supplementary information (ESI) available. CCDC 2203351. For ESI and crystallographic data in CIF or other electronic format see DOI: https://doi.org/10.1039/d3ra00395g

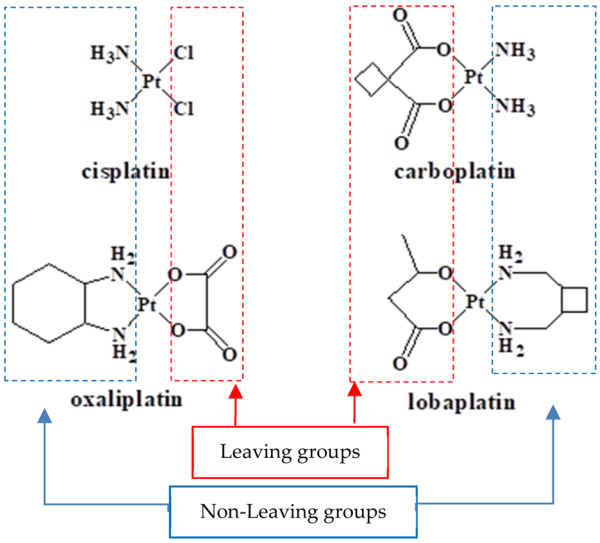

Fig. 1 Some of the clinically approved Pt-based anticancer drugs, illustrating the ligand roles.

platinum(II)-based drugs[11] (Fig. 1), all of which act by a mechanism similar to that of cisplatin. However, the use of bidentate leaving groups in these complexes has been found to kinetically slow the activation process compared to cisplatin, reducing the efficacy.[12]

In the search for more efficient/less toxic platinum(II) candidates, attention has focused on complexes that bind to DNA non-covalently, including *via* electrostatic, groove and intercalation interactions. Terpyridine and its derivatives have been employed as good intercalating ligands in designing Pt(II) complexes. For instance, binding studies of the complex $[Pt(tpy)Cl]^+$ have suggested fast intercalation of the ligand with DNA which is followed by chlorido/$N_{nucleobase}$ ligand exchange (loss of the labile chlorido ligand).[13–17] In contrast, complexes with the formula $[Pt(tpy)(thiol)]^+$ demonstrate DNA-binding *via* intercalation exclusively. The thiols are poorer leaving groups than chlorido, and some of these complexes have shown promising *in vitro* cytotoxicity.[18,19] Other ligands have been used to generate platinum(II) complexes, resulting in complexes that can bind DNA covalently and through intercalation.[20–22]

In a recent article, we described the synthesis of Pt(N^N^O)Cl complexes (Fig. 2), employing tridentate Schiff base ligands synthesized from 2-picolylamine and salicylaldehyde derivatives {3-ethoxy (OEt), 4-diethylamino (NEt_2) and 4-hydroxy (OH)}.[23] The DNA-binding studies of these platinum(II) complexes suggested fast intercalation followed by a slow shift towards covalent binding. Among the platinum(II) complexes, the ethoxy-containing complex exhibited the most promising IC_{50} against both MCF-7 and HepG2 cell lines, and comparable to that observed for cisplatin. DFT calculations for the B-DNA trimer adduct with platinum complexes showed hydrogen bonding interactions between the ligands and nucleobases, affecting the inter-strand hydrogen bonding within the DNA, which highlights the strong ability of the complexes to induce conformational changes in the DNA that lead to the activation of apoptotic cell death, a premise supported by cell cycle arrest studies.[23] The current work is an extension of this recent work; in the synthesis of the ligands, 2-picolylamine has been replaced by *N*-phenyl-1,2-diaminobenzene or *N*-phenyl-1,2-diaminoethane. Such modifications have produced tridentate ligands with variant nitrogen basicity, and hence platinum(II) complexes with different electronic properties (Fig. 2). The effect of the basicity of the nitrogen donating atoms on the DNA-binding and anticancer properties have been studied, and theoretical studies have been undertaken to rationalize the outcomes.

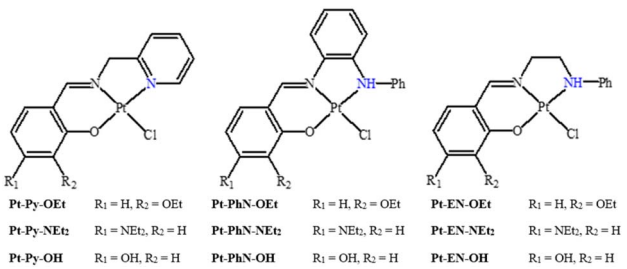

Fig. 2 Platinum(II) compounds in this work.

2 Materials and methods

2.1 Materials

All the reactions were conducted under an inert atmosphere (argon), using standard Schlenk techniques with oven-dried glassware. Molecular sieves (A4) were used to dry all solvents for at least 48 hours before use. Propidium iodide (PI) was purchased from Thermo-Fisher Scientific. All other reagents and chemicals were sourced from Sigma-Aldrich and used as received. *N*-(2-Picolyl)salicylimine ligands (**L-Py-OEt**, **L-Py-NEt2** and **L-Py-OH**) and their platinum(II) complexes (**Pt-Py-OEt**, **Pt-Py-NEt2** and **Pt-Py-OH**) were synthesized according to the previously reported procedure.[23]

2.2 Methods and instrumentation

High-resolution (HR) electrospray ionization (ESI) (positive ionization mode) mass spectra were conducted employing a Bruker Apex 4.7 FTICR-MS instrument; all mass spectrometry (MS) peaks are listed as *m*/*z* (formula). The elemental analyses were carried out at King Abdulaziz University. The infrared (IR) spectra were collected as KBr disks on a PerkinElmer Spectrum 100 instrument; the reported peaks are in cm^{-1}. ^1H NMR (600 MHz), ^{13}C NMR (151 MHz), and ^{31}P NMR (242 MHz) spectra were obtained, using a Bruker Avance 600 MHz spectrometer equipped with a BBO probe; the spectra were referenced to residual chloroform or DMSO (7.26 or 2.50, ^1H), $CDCl_3$ or DMSO-d_6 (77.0 or 39.5 ^{13}C), or external H_3PO_4 (0.0 ^{31}P).[24] Atom labelling in NMR follows the numbering scheme in Chart 1. UV-vis absorption spectra were obtained as chloroform solutions on a Genesys-10s UV-VIS spectrophotometer (Thermo Fischer), using 1 cm path-length quartz cells; the absorption maxima wavelengths are given in nanometres.

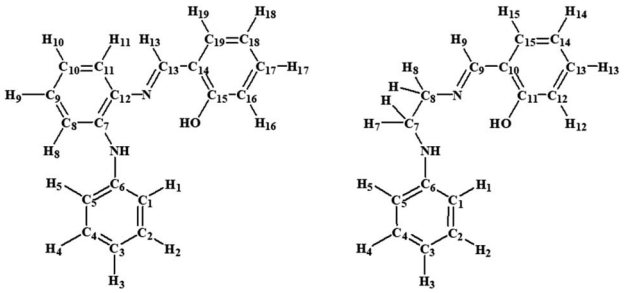

Chart 1 NMR labelling scheme for compounds in the current work.

2.3 Synthesis and characterization

2.3.1 General synthetic procedure for the Schiff base ligands from *N*-phenyl-*o*-phenylenediamine. Equimolar amounts of *N*-phenyl-*o*-phenylenediamine and salicylaldehyde derivatives were stirred at reflux in 10 mL of ethanol for 30 min. The resultant precipitate was collected by filtration, washed with ethanol, and dried under vacuum.

*2.3.1.1 Ligand 1 (**L-PhN-OEt**).* *N*-Phenyl-*o*-phenylenediamine (0.50 g, 2.70 mmol) and 3-ethoxysalicylaldehyde (0.45 g, 2.70 mmol) were reacted to yield L1 as an orange powder (0.71 g, 82%). IR (cm^{-1}): 1622 ν(C=N), 2891–3053 ν(O–H), 3428 ν(aromatic NH). ^{1}H-NMR ($CDCl_3$) δ: 13.18 (s, 1H, OH), 8.59 (s, 1H, H_{13}), 7.26 (d, J_{HH} = 8.1, 2H, $H_{1,5}$), 7.22 (t, J_{HH} = 7.6, 2H, $H_{2,4}$), 7.11 (d, J_{HH} = 7.7, 2H, H_{11}), 7.07 (d, J_{HH} = 7.7, 2H, $H_{17,19}$), 6.97 (d, J_{HH} = 7.7, 2H, H_8), 6.93 (t, J_{HH} = 4.9, 1H, $H_{9,10}$), 6.82 (q, J_{HH} = 8.0, 1H, $H_{3,18}$), 6.15 (s, 1H, NH), 4.06 (q, J_{HH} = 7.0, 2H, CH_2), 1.43 (t, J_{HH} = 7.0, 3H, CH_3). ^{13}C-NMR ($CDCl_3$) δ: 162.9 (C_{13}), 151.0 (C_{15}), 147.7 (C_{16}), 141.9 (C_{12}), 138.0 (C_7), 136.9 (C_6), 129.3 ($C_{2,4}$), 127.9 (C_{11}), 123.9 ($C_{9,10}$), 122.3 (C_{19}), 120.2 ($C_{1,5}$), 119.6 (C_{14}), 118.9 (C_{17}), 118.7 (C_3), 116.2 (C_{18}), 115.2 (C_8), 64.6 (CH_2), 14.9 (CH_3). HR ESI MS calcd for $[C_{21}H_{20}N_2O_2]^+$: 332.1525, found 332.1462. Anal. calcd for $C_{21}H_{20}N_2O_2$: C, 75.88; H, 6.06; N, 8.43%; found: C, 76.21; H, 5.79; N, 8.06%.

*2.3.1.2 Ligand 2 (**L-NPh-NEt$_2$**).* *N*-Phenyl-*o*-phenylenediamine (0.50 g, 2.70 mmol) and 4-diethylaminosalicylaldehyde (0.52 g, 2.70 mmol) were reacted to yield L2 as a yellow powder (0.74 g, 76%). IR (cm^{-1}):1600 ν(C=N), 2819–3140 ν(O–H), 3386 ν(aromatic NH). ^{1}H-NMR (d^6-DMSO) δ: 13.13 (s, 1H, OH), 8.59 (s, 1H, H_{13}), 7.25 (d, J_{HH} = 5.9, 1H, H_1), 7.23 (d, J_{HH} = 5.8, 1H, H_5), 7.18 (t, J_{HH} = 5.8, 2H, $H_{2,4}$), 7.11 (t, J_{HH} = 5.5, 1H, H_9), 7.32 (d, J_{HH} = 6.6, 1H, H_8), 7.48 (s, 1H, H_{16}), 6.98 (d, J_{HH} = 5.8, 1H, H_{11}), 6.77 (t, J_{HH} = 5.5, 1H, H_{10}), 6.30 (dd, J_{HH} = 1.7, 1H, H_3), 6.02 (d, J_{HH} = 1.6, 1H, $H_{18,19}$), 3.38 (q, J_{HH} = 5.3, 2H, CH_2), 1.12 (t, J_{HH} = 5.2, 3H, CH_3). ^{13}C-NMR (d^6-DMSO) δ: 162.9 (C_{13}), 161.0 (C_{15}), 151.2 (C_6), 144.2 (C_{12}), 140.5 (C_7), 136.4 (C_9), 133.9 ($C_{2,4}$), 128.9 ($C_{8.11}$), 125.8 (C_{10}), 121.9 (C_{19}), 119.1 ($C_{1,5}$), 119.0 (C_3), 109.1 (C_{18}), 103.5 (C_{16}), 96.8 (C_{14}), 43.8 (CH_2), 12.4 (CH_3). HR ESI MS calcd for $[C_{23}H_{25}N_3O]^+$: 360.2076, found 360.2070. Anal. calcd for $C_{23}H_{26}N_3O$: C, 76.85; H, 7.01; N, 11.69%; found: C, 76.57; H, 6.59; N, 11.35%.

*2.3.1.3 Ligand 3 (**L-NPh-OH**).* *N*-Phenyl-*o*-phenylenediamine (0.50 g, 2.70 mmol) and 2,4-dihydroxybenzaldehyde (0.37 g, 2.70 mmol) were reacted to yield L3 as an orange powder (0.73 g, 88%). IR (cm^{-1}): 1630 ν(C=N), 2781–3289 ν(O–H), 3437 ν(aromatic NH). ^{1}H-NMR ($CDCl_3$) δ: 11.40 (s, 1H, OH), 9.69 (s, 1H, OH), 8.43 (s, 1H, H_{13}), 7.40 (d, J_{HH} = 6.4, 2H, $H_{1,5}$), 7.33 (d, J_{HH} = 5.9, 2H, H_8), 7.21 (t, J_{HH} = 4.1, 2H, H_2), 7.17 (t, J_{HH} = 5.6, 1H, H_4), 7.06 (d, J_{HH} = 5.8, 1H, H_{11}), 6.99 (t, J_{HH} = 5.6, 1H, H_9), 6.90 (t, J_{HH} = 5.6, 1H, H_{10}), 6.60 (s, 1H, H_{16}), 6.48 (dd, J_{HH} = 1.6, 1H, H_3), 6.39 (d, J_{HH} = 1.6, 1H, $H_{18,19}$). ^{13}C-NMR ($CDCl_3$) δ: 164.7 (C_{13}), 163.4 ($C_{15,17}$), 137.0 ($C_{12,19}$), 136.1 ($C_{6,7}$), 129.3 ($C_{2,4}$), 127.7 ($C_{8,11}$), 121.6 (C_3), 118.9 ($C_{1,5}$), 115.5 ($C_{9,10}$), 108.7 (C_{14}), 103.6 (C_{18}), 103.2 (C_{16}). HR ESI MS calcd for $[C_{19}H_{16}N_2O_2]^+$: 305.1290, found 305.1279. Anal. calcd for $C_{19}H_{16}N_2O_2$: C, 74.98; H, 5.30; N, 9.20%; found: C, 74.72; H, 5.20; N, 9.39%.

2.3.2 General synthetic procedure for the Schiff base ligands from *N*-phenylethylenediamine. Equimolar amounts of *N*-phenylethylenediamine and salicylaldehyde derivatives were stirred at room temperature in 10 mL of hexane. The resultant precipitate was collected by filtration, washed with hexane and dried under vacuum.

*2.3.2.1 Ligand 4 (**L-EN-OEt**).* *N*-Phenylethylenediamine (0.50 g, 3.62 mmol) and 3-ethoxysalicylaldehyde (0.60 g, 3.62 mmol) reacted to yield L4 as a yellow powder (0.71 g, 92%). IR (cm^{-1}): 1587 ν(C=C), 1647 ν(C=N aromatic), 3402 ν(NH). ^{1}H-NMR (d^6-DMSO) δ: 13.66 (s, 1H, OH), 8.48 (s, 1H, H_9), 7.07 (t, J_{HH} = 5.8, 1H, H_2), 6.99 (t, J_{HH} = 5.5, 1H, H_4), 6.76 (t, J_{HH} = 2.3, 1H, H_3), 6.60 (d, J_{HH} = 6.0, 2H, $H_{1,5}$), 6.53 (t, J_{HH} = 5.4, 1H, H_{14}), 5.07 (s, 1H, NH), 4.04 (q, J_{HH} = 5.2, 2H, CH_2), 3.77 (t, J_{HH} = 6.6, 1H, H_7), 3.34 (t, J_{HH} = 4.6, 1H, H_8), 1.33 (t, J_{HH} = 5.2, 3H, CH_3). ^{13}C-NMR (d^6- DMSO) δ: 166.8 (C_9), 152.1 (C_{11}), 148.4 (C_{12}), 147.1 (C_6), 128.8 ($C_{2,4}$), 123.28 (C_3), 123.26 (C_{12}), 118.4 (C_{14}), 117.4 (C_{13}), 116.2 ($C_{1,5}$), 111.9 ($C_{10,15}$), 63.9 (C_7), 56.8 (C_8), 43.4 (CH_2), 14.7 (CH_3). HR ESI MS $[C_{17}H_{20}N_2O_2]^+$: calcd 284.1525, found 284.1722. Anal. calcd for $C_{17}H_{20}N_2O_2$: C, 71.81; H, 7.07; N, 9.85%; found: C, 71.49; H, 6.85; N, 9.62%.

*2.3.2.2 Ligand 5 (**L-EN-NEt$_2$**).* *N*-Phenylethylenediamine (0.50 g, 3.62 mmol) and 4-diethylaminosalicylaldehyde (0.70 g, 3.62 mmol) reacted to yield L5 as a yellow powder (0.71 g, 83%). IR (cm^{-1}): 1508 ν(C=C), 1589 ν(C=N aromatic), 1612 ν(C=N aliph.), 3411 ν(NH). ^{1}H-NMR (d^6-DMSO) δ: 13.54 (s, 1H, OH), 8.17 (s, 1H, H_9), 7.07 (t, J_{HH} = 4.3, 2H, $H_{2,4}$), 6.59 (d, J_{HH} = 5.9, 2H, $H_{1,5}$), 6.52 (t, J_{HH} = 5.3, 1H, H_3), 6.16 (dd, J_{HH} = 1.3 and 6.5, 1H, H_{14}), 5.92 (d, J_{HH} = 1.1, 1H, H_{15}), 5.67 (s, 1H, H_{12}), 3.64 (t, J_{HH} = 4.6, 2H, H_7), 3.28 (t, J_{HH} = 4.1, 1H, H_8), 3.34 (t, J_{HH} = 5.2, 2H, CH_2), 1.10 (t, J_{HH} = 5.3, 3H, CH_3). ^{13}C-NMR (d^6-DMSO) δ: 165.3 (C_9), 164.5 (C_{11}), 150.9 (C_{13}), 148.5 (C_6), 133.0 (C_{15}), 128.8 ($C_{2,4}$), 115.6 (C_3), 111.9 ($C_{1,5}$), 107.8 (C_{10}), 102.7 (C_{14}), 97.3 (C_{12}), 55.6 ($C_{7,8}$), 43.7 (CH_2), 12.5 (CH_3). HR ESI MS $[C_{19}H_{26}N_3O]^+$: calcd 312.2075, found 312.2070. Anal. calcd for $C_{19}H_{25}N_3O$: C, 73.28; H, 8.09; N, 13.49%; found: C, 72.94; H, 7.81; N, 13.19%.

*2.3.2.3 Ligand 6 (**L-EN-OH**).* *N*-Phenylethylenediamine (0.50 g, 3.62 mmol) and 2,4-dihydroxybenzaldehyde (0.49 g, 3.62 mmol) reacted to yield L6 as a yellow powder (0.79 g, 92%). IR (cm^{-1}): 1595 ν(C=C), 1639 ν(C=N aromatic), 3436 ν(NH). ^{1}H-NMR ($CDCl_3$) δ: 7.83 (s, 1H, H_9), 7.14 (t, J_{HH} = 5.8, 1H, $H_{2,4}$), 6.89 (d, J_{HH} = 6.4, 1H, $H_{1,5}$), 6.70 (t, J_{HH} = 5.5, 1H, H_3), 6.59 (d, J_{HH} = 5.9, 2H, H_{15}), 6.23 (s, 1H, H_{12}), 6.22 (dd, J_{HH} = 1.50 and 6.42, 1H, H_{14}), 3.67 (t, J_{HH} = 4.1, 2H, H_7), 3.44 (t, J_{HH} = 4.1, 2H, H_8). ^{13}C-NMR ($CDCl_3$) δ: 164.6 (C_9), 163.6 ($C_{11,13}$), 147.2 (C_6),

134.3 (C_{15}), 129.3 ($C_{2,\ 4}$), 117.9 (C_3), 111.1 ($C_{1,5}$), 107.2 (C_{14}), 104.2 (C_{12}), 54.0 (C_8), 44.0 (C_9). HR ESI MS $[C_{15}H_{16}N_2O_2]^+$: calcd 256.1212, found 256.1254. Anal. calcd for $C_{17}H_{20}N_2O_2$: C, 71.81; H, 7.09; N, 9.85%; found: C, 71.58; H, 6.98; N, 9.56%.

2.3.3 General synthetic procedure for the Pt(II) complexes. A clear solution of K_2PtCl_4 in 1 mL DMSO and 5 mL of methanol was added to a refluxing methanolic solution (15 mL) of equimolar amounts of the ligand (L1–L6) and sodium acetate. The reaction mixture was stirred at reflux for 24 h. Then, the mixture volatiles were evaporated to the minimum volume, and diethyl ether (10 mL) was added, leading to precipitation of the crude product, which was collected, dissolved in the minimum amount of dichloromethane, and filtered into diethyl ether, providing the pure product.

2.3.3.1 ***Pt-NPh-OEt.*** K_2PtCl_4 (100 mg, 0.241 mmol) and L-NPh-OEt (80 mg, 0.241 mmol) reacted to yield Pt-NPh-OEt as a green powder (0.119 g, 88%). IR (cm^{-1}): 1517 ν(C=C), 1604 ν(C=N aromatic), 3437 ν(C=N aliph.). ^{1}H-NMR (d^6-DMSO) δ: 8.58 (s, 1H, H_{13}), 7.62 (d, J_{HH} = 5.4, 2H, $H_{1,5}$), 7.47 (t, J_{HH} = 5.4, 2H, $H_{2,4}$), 7.44 (t, J_{HH} = 7.8, 1H, H_9), 7.37 (t, J_{HH} = 7.5, 1H, H_{10}), 7.14 (d, J_{HH} = 8.2, 2H, $H_{8,11}$), 6.82 (d, J_{HH} = 5.7, 1H, H_{17}), 6.33 (q, J_{HH} = 8.9, 1H, $H_{3,18}$), 3.98 (q, J_{HH} = 6.9, 2H, CH_2), 1.34 (t, J_{HH} = 6.9, 3H, CH_3). ^{13}C-NMR (d^6-DMSO) δ: 157.0 (C_{13}), 150.9 (C_{15}), 146.5 (C_{16}), 138.3 (C_{12}), 136.4 (C_7), 135.3 (C_6), 129.8 ($C_{2,4}$), 127.6 (C_{11}), 124.8 ($C_{9,10}$), 123.9 (C_{19}), 120.7 ($C_{1,5}$), 118.6 (C_{14}), 116.4 (C_3), 116.2 (C_{17}), 114.5 (C_{18}), 111.1 (C_8), 63.4 (CH_2), 14.7 (CH_3). HR ESI MS calcd for $[C_{21}H_{22}N_2O_2ClPt]^+$: 564.1018, found 564.4267. Anal. calcd for $C_{21}H_{19}ClN_2O_2Pt$: C, 44.89; H, 3.41; N, 4.99%; found: C, 44.51; H, 3.14; N, 5.23%.

2.3.3.2 ***Pt-NPh-NEt$_2$.*** K_2PtCl_4 (100 mg, 0.241 mmol) and **L-NPh-NEt$_2$** (86 mg, 0.241 mmol) reacted to yield **Pt-NPh-NEt$_2$** as an orange powder (0.118 g, 83%). IR (cm^{-1}): 1610 ν(C=C), 1603 ν(C=N aromatic), 3448 ν(NH). ^{1}H-NMR (d^6-DMSO) δ: 9.97 (s, 1H, NH), 8.52 (s, 1H, H_{13}), 8.09 (d, J_{HH} = 8.5, 1H, H_{11}), 7.42 (d, J_{HH} = 9.2, 2H, $H_{1,5}$), 7.35 (t, J_{HH} = 7.7, 1H, H_3), 7.30 (t, J_{HH} = 8.0, 2H, $H_{9,10}$), 7.18 (d, J_{HH} = 8.2, 1H, H_{19}), 7.12 (t, J_{HH} = 7.4, 2H, $H_{2,4}$), 6.89 (d, J_{HH} = 7.9, 1H, $H_{8,11}$), 6.29 (d, J_{HH} = 9.2, 1H, H_{18}), 5.90 (s, 1H, H_{16}), 3.36 (q, J_{HH} = 7.3, 2H, CH_2), 1.11 (t, J_{HH} = 7.0, 3H, CH_3). ^{13}C-NMR (d^6-DMSO) δ: 166.1 (C_{13}), 154.5 (C_{15}), 150.2 (C_6), 148.8 (C_{12}), 148.2 (C_7), 142.0 (C_9), 137.2 ($C_{2,4}$), 129.3 ($C_{8,11}$), 127.7 (C_{10}), 127.2 (C_{19}), 126.0 ($C_{1,5}$), 116.5 (C_3), 112.3 (C_{18}), 105.1 (C_{16}), 97.8 (C_{14}), 44.5 (CH_2), 13.2 (CH_3). HR ESI MS calcd for $[PtC_{23}H_{25}N_3OCl]^+$: 589.1334, found 589.1239. Anal. calcd for $C_{23}H_{24}ClN_3OPt$: C, 46.90; H, 4.11; N, 7.13%; found: C, 47.43; H, 4.39; N, 6.59%.

2.3.3.3 ***Pt-NPh-OH.*** K_2PtCl_4 (100 mg, 0.241 mmol) and **L-NPh-OH** (73 mg, 0.241 mmol) reacted to yield **Pt-NPh-OH** as a blue powder (0.096 g, 75%). IR (cm^{-1}): 1525 ν(C=C), 1636 ν(C=N aromatic), 3453 ν(NH). ^{1}H-NMR (d^6-DMSO) δ: 10.33 (s, 1H, NH), 9.36 (s, 1H, OH), 7.99 (s, 1H, H_{13}), 7.63 (t, J_{HH} = 7.6, 1H, H_2), 7.54 (d, J_{HH} = 7.3, 2H, $H_{1,5}$), 7.48 (t, J_{HH} = 7.3, 1H, H_4), 7.14 (d, J_{HH} = 8.3, 1H, H_{18}), 7.02 (d, J_{HH} = 7.2, 1H, H_8), 6.98 (t, J_{HH} = 7.1, 1H, H_9), 6.77 (d, J_{HH} = 7.4, 1H, H_{11}), 6.74 (d, J_{HH} = 8.6, 1H, H_{19}), 6.67 (q, J_{HH} = 6.4, 1H, H_3), 6.46 (t, J_{HH} = 7.0, 1H, H_{10}), 6.15 (d, J_{HH} = 8.3, 1H, H_{11}).^{13}C-NMR ($CDCl_3$) δ: 155.9 (C_{13}), 154.4 ($C_{15,17}$), 148.7 ($C_{11,19}$), 148.1 ($C_{6.7}$), 129.4 (C_{11}), 129.0 ($C_{2,4}$), 127.5 (C_8), 127.0 (C_3), 125.8 ($C_{1,5}$), 123.3 ($C_{9,10}$), 120.5 (C_{14}), 116.3 (C_{18}), 115.4 (C_{16}). HR ESI MS calcd for $[C_{19}H_{15}N_2O_2ClPt]^+$: 531.0314, found 531.4069. Anal. calcd for $C_{19}H_{15}ClN_2O_2Pt$: C, 42.75; H, 2.83; N, 5.25%; found: C, 42.96; H, 2.56; N, 4.89%.

2.3.3.4 ***Pt-EN-OEt.*** K_2PtCl_4 (100 mg, 0.241 mmol) and **L-EN-OEt** (68 mg, 0.241 mmol) reacted to yield **Pt-EN-OEt** as a greenish yellow powder (0.103 g, 84%). IR (cm^{-1}): 1577 ν(C=C), 1612 ν(C=N aromatic), 3490 ν(NH). ^{1}H-NMR (d^6-DMSO) δ: 8.91 (s, 1H, NH), 8.51 (s, 1H, H_9), 7.77 (d, J_{HH} = 7.9, 2H, H_{15}), 7.63 (d, J_{HH} = 7.7, 1H, H_{13}), 7.45 (t, J_{HH} = 7.5, 1H, H_2), 7.37 (t, J_{HH} = 7.9, 1H, H_4), 7.25 (t, J_{HH} = 7.0, 1H, H_3), 7.11 (d, J_{HH} = 8.1, 1H, H_1), 7.00 (d, J_{HH} = 6.3, 1H, H_5), 6.49 (t, J_{HH} = 7.8, 1H, H_{14}), 3.97 (q, J_{HH} = 6.8, 2H, CH_2), 2.99 (t, J_{HH} = 6.7, 1H, H_7), 2.78 (t, J_{HH} = 5.6, 1H, H_8), 1.25 (t, J_{HH} = 7.0, 3H, CH_3). ^{13}C-NMR (d^6-DMSO) δ: 153.7 (C_9), 153.6 (C_{11}), 150.5 (C_{12}), 148.1 (C_6), 129.1 (C_{10}), 127.1 (C_{15}), 125.9 (C_{12}), 124.4 (C_{14}), 122.2 (C_{13}), 117.0 ($C_{1,5}$), 115.3 (C10), 111.9 (C15), 64.5 (C_8), 61.8 (C_7), 60.7 (CH_2), 15.4 (CH_3). HR ESI MS $[C_{17}H_{20}N_2O_2Pt]^+$: calcd 514.0861, found 514.0856. Anal. calcd for $C_{17}H_{19}N_2O_2Pt$: C, 39.73; H, 3.73; N, 5.45%; found: C, 39.27; H, 3.31; N, 4.99%.

2.3.3.5 ***Pt-EN-NEt2.*** K_2PtCl_4 (100 mg, 0.241 mmol) and **L-EN-NEt$_2$** (75 mg, 0.241 mmol) reacted to yield **Pt-EN-NEt$_2$** as an orange powder (0.103 g, 79%). IR (cm^{-1}): 1525 ν(C=C), 1604 ν(C=N aromatic), 3446 ν(NH). ^{1}H-NMR (d^6-DMSO) δ: 9.27 (s, 1H, NH), 8.69 (s, 1H, H_9), 8.16 (d, J_{HH} = 3.1, 1H, H_1), 7.73 (d, J_{HH} = 7.3, 1H, H_5), 7.59 (d, J_{HH} = 7.5, 1H, H_{14}), 7.44 (t, J_{HH} = 7.4, 1H, H_2), 7.35 (t, J_{HH} = 7.4, 1H, H_4), 7.24 (t, J_{HH} = 7.0, 1H, H_3), 7.21 (t, J_{HH} = 9.2, 1H, H_3), 6.34 (d, J_{HH} = 8.8, 1H, H_{15}), 6.23 (s, 1H, H_{12}), 6.15 (d, J_{HH} = 7.1, 1H, H_{14}), 3.83 (t, J_{HH} = 7.3, 2H, $H_{7,8}$), 2.73 (q, J_{HH} = 3.9, 2H, CH_2), 1.09 (t, J_{HH} = 6.7, 3H, CH_3). ^{13}C-NMR (d^6-DMSO) δ: 162.9 (C_9), 156.4 (C_{11}), 153.4 (C_{13}), 151.7 (C_6), 147.6 (C_{15}), 146.4 (C_4), 135.8 (C_3), 134.5 (C_2), 128.5 (C_1), 123.7 (C_5), 111.6 (C_{10}), 103.3 (C_{14}), 98.3 (C_{12}), 60.3 ($C_{7,8}$), 43.7 (CH_2), 12.5 (CH_3). HR ESI MS calcd for $[C_{19}H_{26}ClN_3OPt]^+$: 541.1391, found 541.1310. Anal. calcd for $C_{19}H_{24}ClN_3OPt$: C, 42.19; H, 4.47; N, 7.77%; found: C, 41.84; H, 4.20; N, 7.34%.

2.3.3.6 ***Pt-EN-OH.*** K_2PtCl_4 (100 mg, 0.241 mmol) and **L-EN-OH** (62 mg, 0.241 mmol) reacted to yield **Pt-EN-OH** as a greenish yellow powder (0.096 g, 82%). IR (cm^{-1}): 1543 ν(C=C), 1639 ν(C=N aromatic), 3428 ν(NH). ^{1}H-NMR (d^6-DMSO) δ: 9.85 (s, 1H, OH), 8.07 (s, 1H, H_7), 7.95 (d, J_{HH} = 3.6, 1H, H_{14}), 7.82 (s, 1H, H_{12}), 7.58 (d, J_{HH} = 5.9, 1H, H_{15}), 7.51 (d, J_{HH} = 5.8, 2H, $H_{1,5}$), 7.34 (t, J_{HH} = 5.7, 1H, H_2). 7.20 (t, J_{HH} = 5.3, 1H, H_4), 6.12 (t, J_{HH} = 6.5, 1H, H_3), 5.60 (s, 1H, NH), 2.83 (t, J_{HH} = 7.1, 2H, H_7), 2.86 (t, J_{HH} = 5.5, 2H, H_8). ^{13}C-NMR (d^6-DMSO) δ: 164.8 (C_9), 163.6 (C_{13}), 157.7 (C_{11}), 147.2 (C_6), 135.7 (C_{15}), 128.3 ($C_{2,4}$), 126.0 (C_{14}), 123.6 (C_3), 113.5 ($C_{1,5}$), 105.9 (C_{10}), 103.4 (C_{12}), 59.3 (C_7), 44.9 (C_8). HR ESI MS $[C_{15}H_{16}ClN_2O_2Pt]^+$: calcd 486.0527, found 486.0543. Anal. calcd for $C_{15}H_{15}ClN_2O_2Pt$: C, 37.08; H, 3.11; N, 5.77%; found: C, 36.85; H, 2.79; N, 5.62%.

2.3.4 Crystallographic structure determination. Single crystals of L-EN-NEt$_2$ were grown by vapor diffusion of diethyl ether into a saturated solution of the compound in chloroform. An appropriate single crystal was chosen and mounted on a Bruker APEX2 microsource diffractometer. The crystal was kept at 120.00 K during data collection, using Mo Kα (λ = 0.71073) radiation. Using Olex2,[24] the structure was solved with the SHELXT[25] structure solution program using the intrinsic

Table 1 .Crystal data and structure refinement for L-EN-NEt_2

Empirical formula	$C_{19}H_{25}N_3O$
Formula weight	311.42
Crystal system, space group	Triclinic, $P\bar{1}$
a, b, c (Å)	10.7397(8), 10.9415(9), 16.0325(12)
α, β, γ (°)	88.444(3), 72.754(3), 70.469(3)
Volume (Å^3)	1690.3(2)
Z	4
ρ_{calc} (g cm^{-3})	1.224
μ (mm^{-1})	0.077
F(000)	672.0
Crystal size (mm^3)	0.407 × 0.317 × 0.14
2θ range for data collection (°)	3.962 to 55.032
Index ranges	$-13 \le h \le 13$, $-14 \le k \le 14$, $-20 \le l \le 20$
Reflections collected	59 881
Independent reflections	7752 [$R_{int} = 0.0477$, $R_{sigma} = 0.0256$]
Data/restraints/parameters	7752/0/419
Goodness-of-fit on F^2	1.046
Final R indexes [$I \ge 2\sigma(I)$]	R1 = 0.0465, wR2 = 0.1163
Final R indexes [all data]	R1 = 0.0625, wR2 = 0.1318
Largest diff. Peak/hole (e Å^{-3})	0.62/−0.61

phasing method and refined with the SHELXL[26] refinement package using least squares minimization. Table 1 summarizes the crystal structure refinement details.

2.4 DNA-binding studies

2.4.1 Competitive fluorescence quenching of ethidium bromide-DNA adduct. An aqueous solution of 100 μM ct-DNA/10 μM ethidium bromide (EB) was prepared in Tris–HCl/EDTA buffer system (pH = 7.3). After 24 h incubation time, solutions were obtained from the ct-DNA-EB stock solution, keeping the concentration of ct-DNA/EB constant and changing the concentrations of the platinum complexes (DMSO was used in *ca.* 10% V/V to dissolve the platinum compounds in the buffer). The changes induced by the different concentrations of the platinum complexes on the emission spectra of the ct-DNA-EB adduct were followed between 500 nm and 750 nm upon excitation at 390 nm after incubating the complexes for 5 min. The Stern–Volmer quenching constants (K_{SV}) were obtained from eqn (1) where F_0 and F are the emission intensities in the absence and the presence of the platinum compounds, respectively. The concentration of the platinum complexes was plotted against the ratio of F_0 to F, allowing the extraction of K_{SV} from the slope.[27,28] Apparent binding constants (K_{app}) are obtainable from eqn (2), employing the concentration of the platinum complexes that quenches 50% of the EB fluorescence.[29,30] As we started with 10 μM ethidium bromide and its binding constant (K_{EB}) is 1×10^5,[31] K_{sv} and K_{app} are almost the same. The Stern–Volmer constant is associated to the quenching constant by eqn (3), where K_q is the quenching rate constant, and τ_0 is the average lifetime of the fluorescence for the EB-DNA adduct (τ_0 = 23 ns).[32]

$$F_0/F = 1 + K_{sv}\,[\text{Pt complex}] \quad (1)$$

$$K_{EB}[\text{EB}] = K_{app}\,[\text{Pt complex}]_{50\%} \quad (2)$$

$$K_{sv} = K_q \times \tau_0 \quad (3)$$

2.4.2 Determination of binding mode by changes in relative viscosity of DNA. An Ostwald viscometer was utilized to measure the changes in the relative viscosity of ct-DNA in buffer upon small additions (micro-volumes in the range of 10 μL) of the platinum compounds. After each addition, 10 min incubation time at 25 °C water bath was maintained before the measurement and the ratio of [Pt compounds] to [DNA] was restrained in the range 0.033 to 0.23. The flow times for the solutions were recorded and replicated twice. The plotting of relative viscosity $(\eta/\eta_o)^{1/3}$ against the ratio [Pt compounds]/[DNA] provided a curve, where η_0 and η are defined as the specific viscosity of the free ct-DNA and the ct-DNA-Pt adduct, respectively. The specific viscosity η and η_0 were derived from the formulation $[(t - t_b)/t_b]$ where t is the observed flow time and t_b is the buffer flow time.[28,29,33]

2.5 Assessment of covalent binding of the Pt(II) complexes against guanine

Cisplatin and some platinum(II) based drugs are known to form adducts with DNA through forming coordination bonds with the nitrogen atoms on nucleobases.[2,12] To examine if our platinum(II) complexes are capable of forming nucleobase-adducts, the following procedure was applied: **Pt-Py-OEt** (10 mg, 0.02 mmole) was stirred with equimolar amounts of guanine nucleobase and silver(I) hexafluorophosphate in 10 mL dichloromethane for 24 h. The mixture was filtered to remove the precipitated AgCl. Removal of the solvent afforded a yellow powder. A ^{1}H NMR was obtained and used to evaluate the binding with guanine. The same protocol was adopted for **Pt-EN-OEt** and **Pt-NPh-OEt** with guanine.

2.6 Protein binding studies

Bovine serum albumin (BSA) solution (30 μM) was prepared in Tris–HCl/EDTA aqueous buffer (pH = 7.4). The solution was titrated with different concentrations of the platinum

complexes in DMSO (the amount of DMSO was maintained at *ca.* 20% v/v). The changes in the emission intensity of BSA were tracked at 340 nm upon excitation at 280 nm after incubating the complexes for 30 min at 295 K. The Stern–Volmer quenching constants (K_{SV}) were obtained from eqn (4), where F_0 and F are the intensities of emission of the protein in the absence and the presence of the complexes, respectively. The [Pt complex] was plotted against $[F_0/F]$; the slope of the resultant line was K_{SV}.[29] The Stern–Volmer constant is related to the quenching constant by eqn (5), where K_q is the quenching rate constant, and τ_0 is the average lifetime of the fluorescence for free BSA ($\tau_0 = 5.8$ ns).[34,35] The binding constant (K_b, M^{-1}) and the number of binding sites (n) were obtained by plotting $\log[I_0 - I/I]$ against log[Pt complex], where n equals the slope and $\log(K_b)$ is equivalent to the intercept according to eqn (6).[36] The Gibbs free energy (ΔG^0) of the binding to BSA protein can be estimated by employing eqn (7), using the binding constant (K_b, M^{-1}).[36–38]

$$F_0/F = 1 + K_{sv}[\text{Pt complex}] \quad (4)$$

$$K_{sv} = K_q \times \tau_0{}' \quad (5)$$

$$\log(I_0 - I)/I = \log(K_b) + n(\log[\text{Pt complex}]) \quad (6)$$

$$\Delta G^0 = -\,RT[\ln(K_b)] \quad (7)$$

2.7 Computational studies

The covalent binding properties of the platinum complexes with guanine nucleobase were investigated computationally, employing the Gaussian09 suite.[39] Gaussview software was used for visualization.[40] The density functional theory (DFT) method was implemented with the B3LYP functional[41] with a split-valence double-zeta basis set (6-31G) and five d-type Cartesian-Gaussian polarization functions[42] for all atoms except platinum, for which the SDD basis set was employed.[43] The theoretical calculations were directed to study the energies and structural features of selected [Pt]-Cl and $[\text{Pt-guanine}]^+$ complexes. No symmetry constraints were applied in the geometry optimizations of the Pt-adducts. The final geometries (minimum potential energy structures with no imaginary frequencies) were obtained through frequency calculations. Weak interactions have been implemented in the energy evaluations using Grimme D3 corrections.[44] The delocalization interactions of the proposed complexes were estimated by using the Natural Bond Orbital (NBO) program (Version 3.1).[45]

2.8 Assessments of IC_{50} by MTT assay

Liver (HepG2) and breast (MCF-7) cancer cell lines were provided by the Tissue Culture Unit at the Department of Biochemistry in King Abdulaziz University. Attached cancer cell lines were cultured for 1 day in a flask containing complete media. Dulbecco's Modified Eagle's Medium (DMEM) at 37 °C and 95% humidity in a sterile 5% CO_2 incubator. DMEM were purchased from Life Technologies Gibco. A 0.25% trypsin solution with EDTA (4 mL) was added to the individual cells after 90% of the confluent cells were collected, and placed in a CO_2 incubator for 5 min. The trypsin reaction was ceased by introducing 5 mL of complete medium. The unattached cells containing the medium were then centrifuged, followed by washing the pellets twice with sterile phosphate buffer saline (PBS).[46]

The number of cells was assigned with a hemocytometer and counted in the four major squares after staining 20 μL of this cell-containing media with 20 μL 0.4% trypan blue. A 96-well microplate was equipped with 0.1 mL of 10^4 cells suspended in complete media, and the plate was incubated for 24 h. For each of the platinum coordination compounds, different amounts (3.5, 7, 14, 28, 56 μM) were added to the media when 70% of the cells in each well were confluent. Each concentration was replicated four times. The incubation time for the plate was 48 h.

In each well, the medium was exchanged with 100 μL of 0.5 mg MTT/mL free media for 4 hours in the incubator. Each well was filled with 100 μL DMSO and incubated at room temperature for 15 min before being observed using a Bio-RAD microplate reader at 595 nm. The half maximal inhibitory concentrations (IC_{50}) of the complexes were calculated from the curve of the percentage of cell viability *versus* different concentration of the complex, employing GraphPad prism 9 software.[47]

2.9 Flow cytometry analysis of the cell cycle of HepG2 treated with platinum compounds

The DNA binder propidium iodide was applied in the DNA staining to quantify cellular aggregation in different phases of the cell cycle by flow cytometry.[48] In a 6-well plate, *ca.* 1×10^6 HepG2 cells were seeded for 24 hours. The medium was treated with **Pt-Py-OEt**, **Pt-PhN-OEt** and **Pt-EN-OEt** at IC_{50} concentrations. After 24 h incubation, collection of the treated HepG2 cells was accomplished by the addition of 0.5 mL 0.25% trypsin and then ceasing the activity of trypsin by adding 0.5 mL complete medium to each well. The suspended cells were then centrifuged for 5 min at 1500 rpm followed by washing the cells twice with PBS. The cells were fixed with 1 mL of ethanol (70%) for 4 h at −20 °C. 100 μl of suspended cells with cold PBS with RNase A was then stained with propidium iodide solution (50 mg mL^{-1}) and incubated in the dark for 1 h. All the stained cells were observed, employing a flow cytometer (Applied Biosystem, USA).

3 Results and discussion

3.1 Synthesis and characterization

Schiff bases are normally synthesized *via* the condensation of primary amines and aldehydes. The reaction involves removing water from the hemiaminal intermediate. The reactions of 2-picolylamine and *N*-phenylethylenediamine with different salicylaldehyde derivatives in refluxing absolute ethanol were messy and provided oily mixture of materials. However, the reactions with *N*-phenyl-*o*-phenylenediamine proceeded very

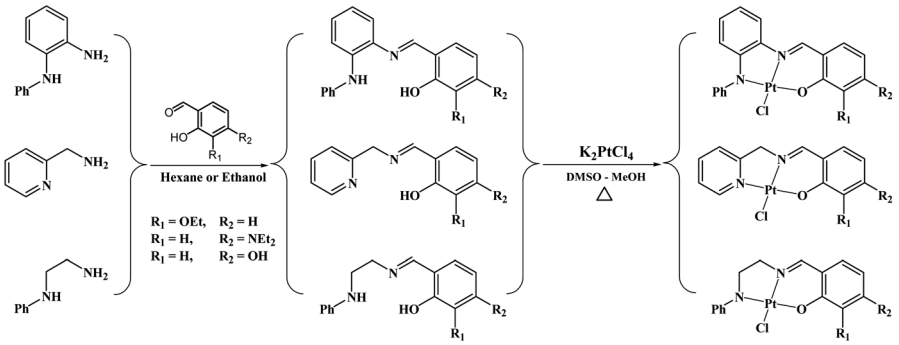

Fig. 3 Synthesis of the ligands and their platinum(II) compounds.

well in refluxing ethanol, precipitating the desired products from the reaction mixture in good yields (Fig. 3). To facilitate the Schiff base formation of 2-picolylamine and *N*-phenylethylenediamine, the precursors were stirred with the aldehydes in hexane, leading to mass precipitation of the desired products (Fig. 3). ^{1}H NMR spectra of the products show the disappearance of the aldehyde signals around 10 ppm and the appearance of the imine signals in the range 7.8–8.8 ppm, confirming reaction progression. Signals in the ^{1}H NMR spectra of the ligands can be divided into three distinctive groups: O–H in the range 10–14 ppm, aromatic protons in the range 6–9.5 ppm and aliphatic protons between 1–5 ppm. When the ligands react with the platinum centre, they produce complexes with ^{1}H NMR data matching the signals pattern of the ligands with slight shifts from that seen in the ligands and the loss of phenolic protons due to the formation of the O–Pt bond (Fig. 3). In particular, the signals of the CH=N are clearly shifted due to the coordination of the nitrogen to the platinum. Mass spectra of all the ligands and complexes exhibit $[M]^+$ or $[M + H]^+$ except Pt–OH which shows $[M–Cl + MeCN]^+$ as the major peak in the spectrum.

3.2 Crystal structure of L-EN-NEt$_2$

The structure of **L-EN-NEt$_2$** has triclinic ($P\bar{1}$) symmetry (Fig. 4). One of the features of the ligand is the absence of delocalization through the imine bond, as the C=N and *N*–CH_2 bond lengths are 1.3036(18)–1.3110(18) Å and 1.4548(17)–1.4576(18) Å, respectively; hence, the lone pair is free for coordination. Intramolecular hydrogen bonding is observed between OH, the nitrogen of the Schiff base, and the nitrogen of the amine. Two different types of intermolecular interactions are responsible for the crystal packing: (a) C_{13}–H···N_5 hydrogen bonding with a distance of 0.99 Å and (b) C_{31}–H···O_1 hydrogen bonding with a distance of 0.99 Å. Other structural data are available in the ESI.†

3.3 DNA-binding studies

While cisplatin covalently binds to DNA, binding studies of $[Pt(tpy)Cl]^+$ have suggested intercalation of the 2,2′; 6′,2″-terpyridine with DNA, followed by covalent bonding between the metal and one of the nucleobases.[49–51] In our recent work, platinum(II) complexes containing *N*-(2-picolyl)salicylimine ligands (**Pt-Py-OEt**, **Pt-Py-NEt$_2$** and **Pt-Py-OH**) were investigated. We concluded that the intercalation mode of binding with DNA changes over time to covalent binding, with **Pt-Py-NEt$_2$** exhibiting the largest apparent binding constant.[23] We explored the binding behavior of the other six complexes with ct-DNA by studying changes in (a) the fluorescence behavior of EB-DNA upon addition of platinum(II) complexes, and (b) the relative viscosity of ct-DNA upon addition of platinum(II) complexes. Ethidium bromide (EB) binds to DNA *via* intercalation, resulting in an intense fluorescent adduct with a wavelength maximum at 590 nm.[52] The platinum(II) complexes act as quenchers by binding with ct-DNA and destabilizing the EB-DNA adduct; hence, its binding behavior was not explored. All the other complexes in the current study can quench the EB-

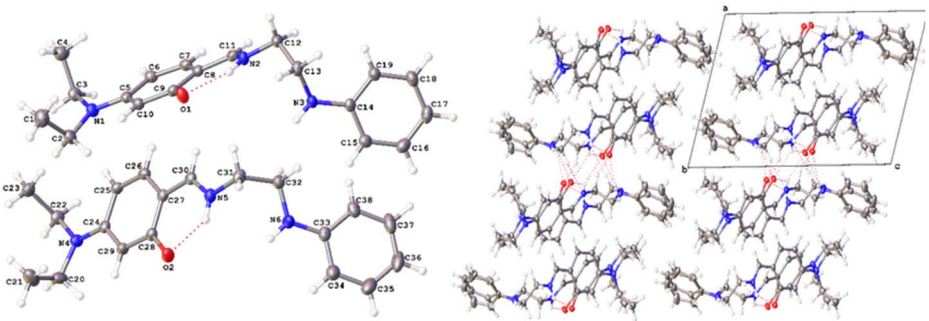

Fig. 4 Crystal structure of L-EN-NEt$_2$.

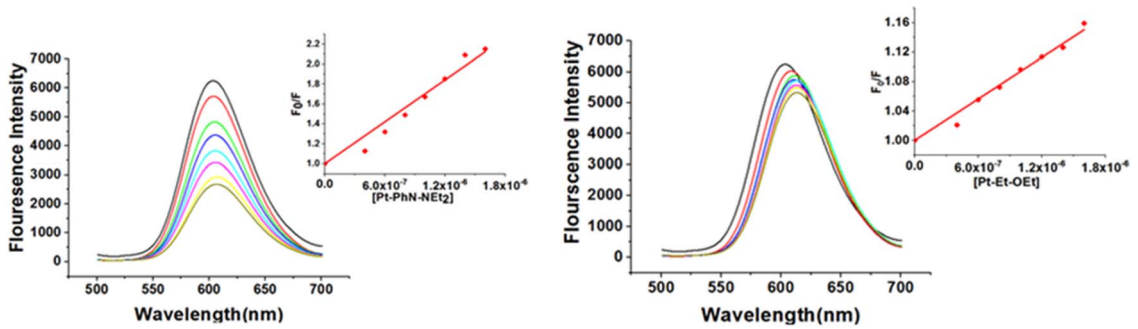

Fig. 5 DNA binding affinities of **Pt-PhN-NEt$_2$** and **Pt-EN-OEt** from fluorescence competitive quenching of the EB-DNA adduct.

DNA adduct to different extents (Fig. 5). The quenching process can be a dynamic process (collisions between the excited fluorophore (EB-DNA) with the quencher) or static process (interaction between the fluorophore and the quencher at the ground state forming a non-fluorescent system). The calculated quenching constants are in the range (4.1–98.9) $\times$ 10^{12} M s^{-1}, indicating a static quenching mechanism (the maximum rate for dynamic quenching is 2.00 $\times$ 10^{10} M s^{-1}).[53] The calculated Stern–Volmer quenching constants (K_{sv}) from eqn (1) are considered as the apparent binding constants (K_{app}) for the complexes and they are listed in Table 2. The values are higher than the apparent binding constant for EB for all the complexes except **Pt-EN-OEt**; pyridine containing complexes possess the highest apparent binding constants, which indicates the importance of the ligand planarity in improving the DNA binding. The other five complexes have binding affinities within the range (0.94–9.89) $\times$ 10^5 M s^{-1}. The quenching with **Pt-EN-OEt** causes a distinct shift of the emission maximum following addition of the complex; this phenomenon was noted previously with **Pt-Py-OEt**.[23] We believe that steric hindrance induced by the ethoxy group causes conformational changes near the EB units and hence modify its emission maximum. The emission quenching of the EB-DNA adduct indicates the strength of the binding, but is not conclusive for the mode of binding adduct. It

Table 2 DNA binding and BSA binding parameters of the different Pt(II) complexes

Complex		Pt-Py-OEt	Pt-Py-NEt$_2$	Pt-Py-OH	Pt-PhN-NEt$_2$	Pt-PhN-OH	Pt-EN-OEt	Pt-EN-NEt$_2$	Pt-EN-OH
DNA-binding	Apparent binding constant (K_{app}) ($\times 10^5$)	(12.5 $\pm$ 4.0)	(20.6 $\pm$ 0.8)	(15.4 $\pm$ 0.9)	(7.02 $\pm$ 0.3)	(5.38 $\pm$ 0.3)	(0.94 $\pm$ 0.4)	(8.38 $\pm$ 0.4)	(9.89 $\pm$ 0.6)
Protein binding	Stern–Volmer constant (K_{sv}) ($\times 10^6$)	6.98	2.92	1.09	2.17	0.89	2.91	2.46	1.57
	Binding constant (K_b) ($\times 10^7$)	2.35	0.125	0.98	0.465	0.062	4.90	0.048	0.175
	Number of binding sites (n)	1.09	0.94	1.16	1.06	0.37	1.2	0.92	1.01
	ΔG^0 (kJ mol^{-1})	−42	−34.8	−39.9	−38.0	−33.0	−43.9	−32.4	−35.3

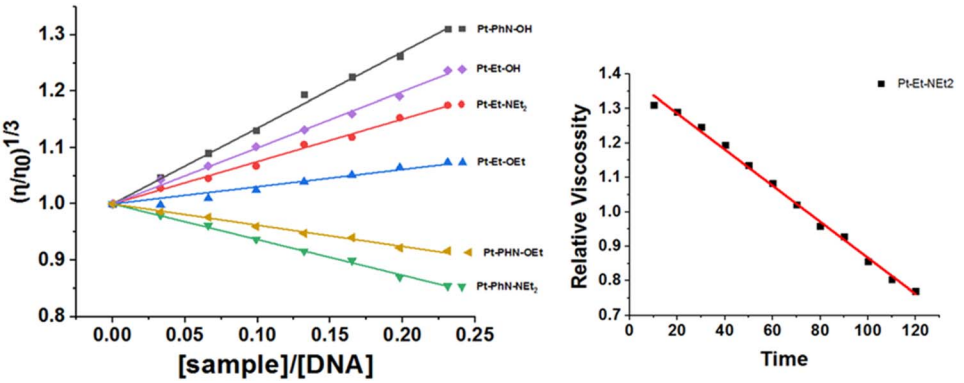

Fig. 6 Changes in relative viscosity of ct-DNA upon treatment with platinum(II) complexes (left). Change in relative viscosity of ct-DNA upon addition of 10 μM **Pt-EN-NEt$_2$** over 120 min (right).

is worth mentioning that **Pt-PhN-OEt** is intensively emissive and its emission overlaps with the emission of the EB-DNA.

The changes in the viscosity of ct-DNA that resulted from adding increasing concentrations of the platinum(II) complexes were monitored, so as to help identify the mode of interaction. After 10 min of mixing, **Pt-PhN-OH**, **Pt-EN-OH**, **Pt-EN-NEt$_2$** and **Pt-EN-OEt** induced increases in the relative viscosity of ct-DNA, as a result of an intercalation mode of interaction[54] (Fig. 6). **Pt-PhN-OH**, **Pt-EN-OH**, **Pt-Py-OH**, **Pt-EN-NEt$_2$**, **Pt-Py-NEt$_2$**, **Pt-EN-OEt**, and **Pt-Py-OEt**, as well as Pt(terpy)Cl, are structurally related complexes and exhibit DNA binding that shifts gradually from the intercalation mode to the covalent binding mode with slow rates of chloride substitution (substantial enough to observe the intercalation: Fig. 6). However, **Pt-PhN-NEt$_2$** and **Pt-PhN-OEt** bind covalently to ct-DNA without the intermediacy of intercalation, leading to reduced relative viscosity as a result of DNA double helix unwinding.[55]

Several platinum(II) complexes including cisplatin are activated *via* chlorido/aqua exchange process.[56] The rate of the aquation process should not be so fast as to activate the anticancer agent before reaching the nuclear DNA.[57] The faster rate of dissociation of the chlorido ligand and the coordination of the ct-DNA in **Pt-PhN-NEt$_2$** and **Pt-PhN-OEt** is clear from the DNA-binding study. Square planar complexes with 16 electron counts are normally inert, with their substitution proceeding slowly. Two factors could be related to the rate enhancement in complexes derived from *N*-phenyl-*o*-phenylenediamine: the ligand bulkiness (the presence of the *N*-phenyl group), and the higher trans effect of the nitrogen of the CH=N bond (compared to the others). In the absence of crystal structures of all the complexes, theoretical studies were conducted to evaluate the structural differences between the various complexes and relate them to the dissociation rate of the chlorido ligand. Optimized structures of **Pt-Py-OEt**, **Pt-Py-NEt$_2$**, **Pt-PhN-OEt**, **Pt-PhN-NEt$_2$**, **Pt-EN-OEt**, and **Pt-EN-NEt$_2$** were obtained (Fig. 7), the important bond lengths and angles being listed in Table 3. In the optimized structures, the most significant difference in bonding is at the Pt–N1 bond (N1 being the nitrogen of the pyridine or of the amine). This bond length increases with the increase in the nitrogen basicity. In term of angles, the N1–Pt–Cl and N2–Pt–O angles are larger than 91° and differ significantly between the complexes, highlighting the role of the pyridine, phenylamine or ethylamine moieties on the molecular geometry. This difference in angles is reflected in the planarity of the molecule and the degree of distortion from square planar that is believed to be responsible for the difference in kinetic liability. Complexes containing the phenylamine fragments show the largest deviation from planarity (distortion from square planar), and exhibit the most labile DNA-covalent binding. The electronic role of the pyridine, phenylamine and ethylamine moieties was also evaluated by NBO (charge) analysis (Table 4). Note that the charge difference (polarity) for the Pt–Cl bond is 0.045 (for **Pt-EN-OEt**), 0.053 (for **Pt-Py-OEt**), and 0.07 (for **Pt-PhN-OEt**). These differences are mainly due to the different charge on the platinum atom of the three complexes. The Pt–Cl

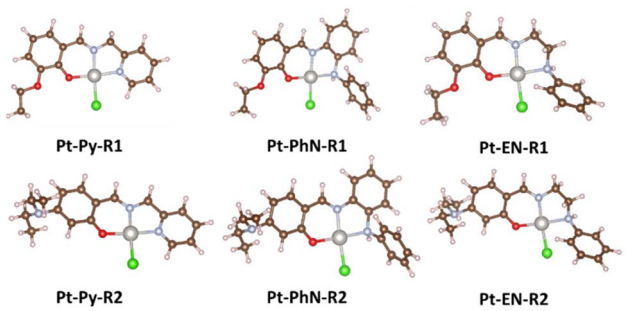

Fig. 7 Optimized structures of the different complexes.

Table 3 Bond lengths and angles of some platinum(II) complexes from theoretical calculations

	Bond lengths (Å)				Angles (°)			Dihedrals (°)	
Complexes	Pt–N1	Pt–N2	Pt–O	Pt–Cl	O–Pt–Cl	N1–Pt–N2	N1–Pt–Cl	Pt–*N*–C–H	O–Pt–*N*–C
Pt-Py-OEt	2.04	2.00	2.01	2.36	89.08	82.28	95.31	−180.00	0.01
Pt-Py-NEt$_2$	2.04	2.00	2.01	2.36	88.89	82.18		179.99	0.14
Pt-PhN-OEt	2.09	2.01	2.01	2.35	91.01	83.29	91.70	178.69	3.96
Pt-PhN-NEt$_2$	2.09	2.02	2.01	2.35	90.86	83.13		177.54	5.48
Pt-EN-OEt	2.12	2.00	2.01	2.35	90.50	83.59	93.21	−179.43	4.44
Pt-EN-NEt$_2$	2.12	2.01	2.01	2.35	90.18	83.49		−179.43	4.36

Table 4 Charges of the coordinating atoms of selected complexes from NBO analysis

	Charge as obtained by NBO analysis					Δ charge
Complex	Pt	O	C=N (Schiff base)	N (pyridine or amine)	Cl	Pt–Cl
Pt-Py-OEt	+0.602	−0.638	−0.585	−0.505	−0.549	+0.053
Pt-PhN-OEt	+0.613	−0.630	−0.591	−0.689	−0.543	+0.070
Pt-EN-OEt	+0.582	−0.640	−0.592	−0.694	−0.537	+0.045

polarity correlates inversely with the rate of the covalent binding in the complexes.

3.4 Assessment of covalent binding of the Pt(II) complexes against guanine

Selected platinum complexes were reacted with guanine, using silver(I) hexafluorophosphate as chloride scavenger. All of these platinum complexes formed complexes with guanine as can be seen from ^{1}H NMR data, but we were unable to conclude which nitrogen on the nucleobases bound to the metal due to: (1) the broadening of the signals in the ^{1}H NMR, (b) the tautomeric nature of the guanine and the presence of only one proton with a strong signal in the ^{1}H NMR, and (c) the low signal-to-noise ratio in the ^{13}C NMR spectra. As a result, theoretical calculations were undertaken to evaluate the preferred nitrogen for binding. Two types of guanine adduct of **Pt-Py-OEt**, **Pt-Py-NEt$_2$**, **Pt-PhN-OEt**, and **Pt-PhN-NEt$_2$** were optimized: N_7-guanine and N_3-guanine. Energy calculations were undertaken assuming weak (noncovalent) interactions (Fig. 8). The N_7-guanine adducts of the pyridyl-containing complexes have lower energies than their N_3-guanine analogues. No hydrogen bonding is observed between the guanine and the tridentate ligand. In contrast, the N_3-guanine adduct is energetically dominant when the phenylamine ligands are present. This is clearly due to the significant hydrogen-bonding between the amino group of the guanine and the phenolic oxygen on the tridentate ligand. Moreover, steric hindrance is observable in the N_7-guanine adduct between the *N*-phenyl group and the carbonyl-oxygen, which enforces a greater twist out of planarity for the guanine. The present theoretical calculations highlight the importance of the tridentate ligand design on the bonding of the guanine to the platinum. Fig. 7. Optimized structures of the different complexes.

3.5 BSA-binding studies

The interaction of drugs with blood plasma proteins is important in their transportation and metabolism. Human serum albumin (HSA) accounts for 55% of the protein in blood plasma.[58,59] The interactions of the complexes with bovine serum albumin (BSA) (as an alternative to HSA) were evaluated by BSA fluorescence quenching (at 335–340 nm), varying the concentration of the platinum(II) complexes at 298 K (Fig. 9). Tryptophan-134 in domain I and tryptophan-212 in domain II are responsible for the fluorescence behavior of the BSA.[60] The binding of our complexes changes the environment around the tryptophan units, leading to fluorescence quenching. There are several possibilities for our complexes to bind either covalently to nearby histidine units or in a noncovalent fashion. The data for eight of the platinum complexes are summarized in Table 2. The emission quenching progresses through either dynamic or static mechanisms. The quenching constants (K_q) reveal a static quenching process, because our compounds have rates much higher (in the range 10^{14}–10^{15}) than the maximum rate for dynamic quenching (2.00×10^{10} M s^{-1}).[53] A static quenching mechanism supports the formation of protein-complex adducts. From the Scatchard equation (eqn 5), the binding constants were extracted, showing values between 4.90×10^7 and 4.8×10^5. This highlights the importance of the ligand structural features on the binding to BSA (Table 2). The ethoxy-containing complexes have better binding constants with BSA. The average binding site "*n*" describes the stoichiometric ratio of the compounds to BSA;[61] all of our complexes interact with BSA at one site. The formation of protein-complex adducts is a spontaneous process, with difference in Gibbs free energies ranging from −32.4 to −42.0 kJ mole^{-1}.

3.6 Preliminary *in vitro* antiproliferative activity

The current work extends our previous work to structurally related complexes;[23] hence, we proceeded with anticancer screening against the same cancer cell lines chosen in our

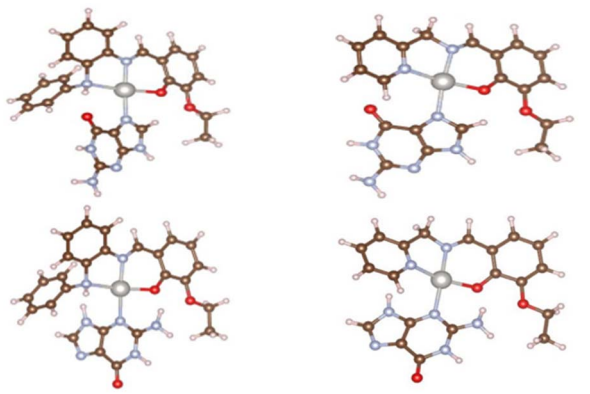

Pt-adduct		Energy (a.u.)	Bonding around the Pt				Hydrogen bonding		ΔE (kcal/mol)
			Pt-N_a	Pt-N_b	Pt-O	Pt-N_G	O-NH_2(G)	H--O_G	
Pt-Py-OEt	N_7-G	-1502.578	2.07	2.02	2.03	2.16	2.26		-7.4
	N_3-G	-1502.590	2.13	2.04	2.14	2.15		2.80	
Pt-Py-NEt_2	N_7-G	-1561.341	2.06	2.00	2.03	2.13	2.45		-6.1
	N_3-G	-1561.350	2.11	2.02	2.13	2.14		2.87	
Pt-PhN-OEt	N_7-G	-1733.656	2.13	2.01	2.02	2.10	2.25		-4.3
	N_3-G	-1733.650	2.16	2.01	2.02	2.15		3.23	
Pt-PhN-NEt_2	N_7-G	-1792.417	2.12	2.00	2.02	2.10	2.34		-3.2
	N_3-G	-1792.411	2.15	2.01	2.03	2.15		3.31	

N_a the nitrogen of the pyridyl or phenylamine
N_b the nitrogen of the Schiff base

Fig. 8 Optimized structures for guanine adducts with structural parameters and energies from theoretical calculations.

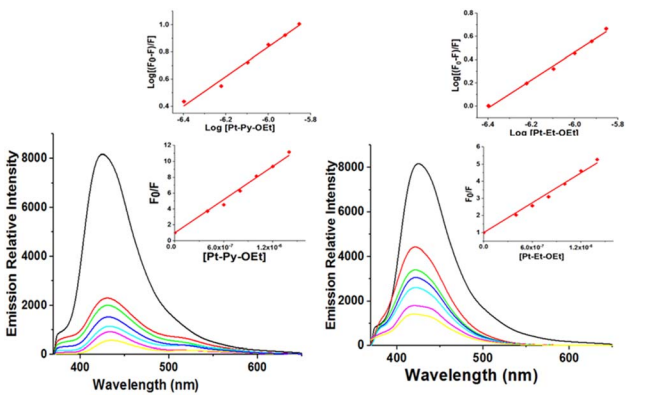

Fig. 9 . Assessment of Protein binding affinities of **Pt-Py-OEt** and **Pt-EN-OEt** by fluorescence quenching.

Table 5 Activities of some platinum(II) complexes and selected ligands against two cancer cell lines

	IC_{50} (μM)	
Compound	HepG2	MCF-7
L-Py-OEt	66.65 ± 6.39	79.57 ± 7.55
L-PhN-OEt	71.18 ± 3.04	97.62 ± 3.09
L-EN-OEt	116.23 ± 9.19	154.84 ± 11.2
Cisplatin	19.73 ± 1.53	18.36 ± 2.72
Pt-Py-OEt	6.99 ± 1.74	13.27 ± 2.10
Pt-PhN-OEt	10.15 ± 0.24	10.97 ± 0.96
Pt-EN-OEt	31.46 ± 0.98	38.96 ± 6.28
Pt-PhN-NEt_2	14.81 ± 0.18	13.96 ± 0.87
Pt-EN-NEt_2	27.14 ± 3.53	28.32 ± 1.27
Pt-PhN-OH	63.87 ± 6.44	66.91 ± 0.88
Pt-EN-OH	77.25 ± 6.43	76.55 ± 4.92

previous work: HepG2 and MCF-7. The IC_{50} values are listed in Table 5 and allow us to extract the following trends:

(1) The minimum inhibitory concentrations for the chosen ligands are relatively poor compared to those of their platinum(II) complexes, highlighting the importance of the platinum in the cytotoxic effects.

(2) Complexes and ligands that contain *N*-phenylethylenediamine are less cytotoxic than their *N*-phenyl-*o*-phenylenediamine and pyridyl containing complexes. The presence of planar aromatic fragments (pyridyl or phenyl) seems to be important for the activity of the complexes.

(3) 4-Hydroxysalicylimine-containing complexes show weak cytotoxic effects compared to the other salicylimine derivatives (3-ethoxy- and 4-diethylamino-containing). The hydroxy group readily dissociates to form a phenoxide moiety, resulting in an overall negative charge on the complex, so DNA binding is electrostatically unfavorable because of the strong repulsion on the backbone.[62]

(4) Three complexes display IC_{50} values significantly less (25% to 65%) than that of cisplatin: **Pt-Py-OEt**, **Pt-PhN-OEt** and **Pt-PhN-NEt_2**. It seems that an ethoxy group at the 3-position of the salicylimine improves the anticancer properties compared to the other two substituents. Deconvoluting the electronic effect of the ethoxy from its steric effect will be addressed in a forthcoming work.

(5) All the examined compounds show slightly better anticancer effects toward the HepG2 cancer cell line compared to the MCF-7 cancer cell line.

3.7 Cell cycle phase analysis of HepG2 treated with selected compounds

The flow cytometry analysis of cell cycle phase distribution was examined for HepG2 cells using PI staining. The cell cycle interference behaviour of **Pt-Py-OEt**, **Pt-PhN-OEt**, and **Pt-EN-OEt** were investigated and compared to that of cisplatin at concentrations around the IC_{50} values of each of the complexes for 24 h. Compared with control cells, treatment of HepG2 cells with cisplatin for 24 h caused an increase in the cell population in the sub-G phase (from *ca.* 1% to 47.3%), with concomitant decreases in the cell population in the G1/G0, S and G2/M phases, suggesting the activation of an apoptotic cell death pathway (Fig. 10). The cell cycle assays of HepG2 treated with **Pt-Py-OEt**, **Pt-PhN-OEt**, and **Pt-EN-OEt** resemble that of HepG2 treated with cisplatin, but with notably different populations in the sub-G (60–65%) and G1/G0 (21–27%) phases (Fig. 10). An apoptotic cell death may be proposed by comparing the similarity in the pattern of the current data of cisplatin and our platinum complexes. Previous literature proposed that the cytotoxic effect of cisplatin is due to DNA damage, involving ATR, p53, p73, and mitogen-activated protein kinases.[63] Our complexes can produce DNA damage by their DNA-binding, although they have only one leaving group (chlorido) compared to two for cisplatin. The ethoxy group causes different conformational changes and activates cell death in ways that differ from that of cisplatin.

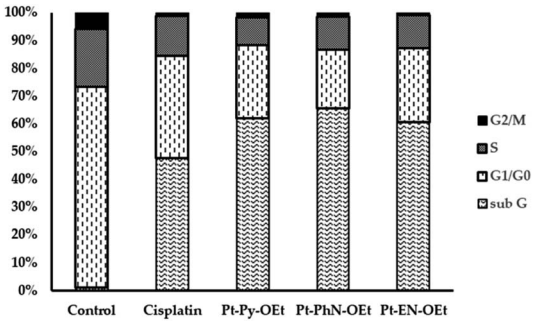

Fig. 10 . Cell cycle assay of HepG2 upon treatment with different compounds.

4 Conclusion

Our recent work on platinum(II) complexes of *N*-(2-picolyl)salicylimine ligands highlighted their promising anticancer activities and the high structural flexibility of the ligands which allow the study of other candidates. In the current work, new ligands were designed by replacing 2-picolylamine with *N*-phenyl-*o*-phenylenediamine and *N*-phenylethylenediamine in the synthesis of tridentate ligands of the type N^N^OH. The new set of ligands were employed in the synthesis of complexes with the formula Pt(N^N^O)Cl. We explored the binding behavior of the complexes with ct-DNA by (a) studying fluorescence quenching behavior of EB-DNA upon addition of the platinum(II) complexes, and (b) studying the changes in relative viscosity of ct-DNA upon addition of the platinum(II) complexes. All the complexes in the current study quench the EB-DNA adduct statically, indicating the formation of complex-DNA adducts. The calculated apparent binding constants (K_{app}) for the pyridine-containing complexes are the highest apparent binding constants, which indicates the importance of the ligand planarity in improving the DNA binding. Moreover, ethoxy-containing complexes induce a distinct shift of the emission maximum of the EB-DNA adduct, presumably indicating the presence of some conformational changes in the DNA structure due to the steric hindrance induced by the ethoxy group. The changes in relative viscosity of ct-DNA indicate that most complexes interact by rapid intercalation, followed by a switch to covalent binding mode over time.

However, **Pt-PhN-NEt2** and **Pt-PhN-OEt** bind covalently without evidence for intercalation at ct-DNA; this difference in behavior, along with the theoretical modeling, stems from the electronic and steric impact of the ligand. The reaction of some platinum complexes with guanine was investigated, revealing a strong tendency to react with guanine; theoretical calculations suggest a strong impact from the tridentate ligand in determining the preferred guanine nitrogen (N3 or N7) to bind the platinum. Similarly, the binding of our complexes with BSA indicated a static interaction with higher binding affinities for the ethoxy-containing complexes. The most critical part of the current study is the anticancer properties. The current data suggest that platinum complexes with tridentate ligands containing a combination of *N*-phenyl-*o*-phenylenediamine or pyridyl with 3-ethoxysalicylimine are good chemotherapeutic candidates. Comparing the cell cycle interference behaviour of cisplatin and our platinum complexes with HepG2 suggests a similar apoptotic cell death. DNA-binding of our complexes produces DNA damage, with conformational changes that depend on the specific ligand, and differences in the activation to cell death from that seen with cisplatin. The current work illustrates the design flexibility of our tridentate ligands and the resultant platinum complexes and highlights the impact of this design flexibility on the anticancer potential. In addition to the good anticancer properties of some of the synthesized platinum complexes, the design flexibility allows more possibilities for the improvement of their physiochemical and pharmacological properties.

Author contributions

Conceptualization, B. A. B.; data curation, K. S. A.; formal analysis, K. S. A., E. M. M. A., B. D., A.-H. M. E. and M. J.; funding acquisition, B. A. B.; investigation, K. S. A. and B. A. B; methodology, K. S. A, A. J., and A.-H. M. E.; project administration, B. A. B.; resources, B. A. B; software, A. J.; supervision, B. A. B.; visualization, K. S. A. and B. A. B; writing–original draft, B. A. B. and M. G. H; writing–review & editing, M. G. H.

Conflicts of interest

The authors declare no conflicts of interest in this publication.

Acknowledgements

This project was funded by the Deanship of Scientific Research (DSR), King Abdulaziz University, Jeddah, Saudi Arabia, under grant no. (KEP-PhD: 36-130-1443). The authors, therefore, acknowledge with thanks DSR technical and financial support. Computation for the work described in this paper was supported by King Abdulaziz University's High-Performance Computing Center (Aziz Supercomputer).

References

1 D. Wang and S. J. Lippard, Cellular processing of platinum anticancer drugs, *Nat. Rev. Drug Discovery*, 2005, **4**, 307–320.
2 D. P. Bancroft, C. A. Lepre and S. J. Lippard, Platinum-195 NMR kinetic and mechanistic studies of cis- and trans-diamminedichloroplatinum(II) binding to DNA, *J. Am. Chem. Soc.*, 1990, **112**, 6860–6871.
3 A. M. Fichtinger-Schepman, J. L. van der Veer, J. H. den Hartog, P. H. Lohman and J. Reedijk, Adducts of the antitumor drug cis-diamminedichloroplatinum(II) with DNA: formation, identification, and quantitation, *Biochemistry*, 1985, **24**, 707–713.
4 U.-M. Ohndorf, M. A. Rould, Q. He, C. O. Pabo and S. J. Lippard, Basis for recognition of cisplatin-modified DNA by high-mobility-group proteins, *Nature*, 1999, **399**, 708–712.
5 Y. Jung and S. J. Lippard, Direct cellular responses to platinum-induced DNA damage, *Chem. Rev.*, 2007, **107**, 1387–1407.
6 P. J. Sadler and Z. Guo, Metal complexes in medicine: design and mechanism of action, *Pure Appl. Chem.*, 1998, **70**, 863–871.
7 M. D. Hall, M. Okabe, D.-W. Shen, X.-J. Liang and M. M. Gottesman, The role of cellular accumulation in determining sensitivity to platinum-based chemotherapy, *Annu. Rev. Pharmacol. Toxicol.*, 2008, **48**, 495–535.
8 H. Timmer-Bosscha, N. H. Mulder and E. G. de Vries, Modulation of cis-diamminedichloroplatinum(II) resistance: a review, *Br. J. Cancer*, 1992, **66**, 227–238.
9 D.-W. Shen, L. M. Pouliot, M. D. Hall and M. M. Gottesman, Cisplatin resistance: a cellular self-defense mechanism resulting from multiple epigenetic and genetic changes, *Pharmacol. Rev.*, 2012, **64**, 706–721.
10 M. M. Gottesman, Mechanisms of cancer drug resistance, *Annu. Rev. Med.*, 2002, **53**, 615–627.
11 K. M. Deo, D. L. Ang, B. McGhie, A. Rajamanickam, A. Dhiman, A. Khoury, J. Holland, A. Bjelosevic, B. Pages, C. Gordon and J. R. Aldrich-Wright, Platinum coordination compounds with potent anticancer activity, *Coord. Chem. Rev.*, 2018, **375**, 148–163.
12 S. P. Fricker, Metal based drugs: from serendipity to design, *Dalton Trans.*, 2007, **43**, 4903–4917.
13 Ž. D. Bugarčić, F. W. Heinemann and R. van Eldik, Substitution reactions of $[Pt(terpy)X]^{2+}$ with some biologically relevant ligands. Synthesis and crystal structure of $[Pt(terpy)(cyst\text{-}S)](ClO_4)_2\cdot 0.5H_2O$ and $[Pt(terpy)(guo\text{-}N^7)](ClO_4)_2\cdot 0.5guo\cdot 1.5H_2O$, *Dalton Trans.*, 2004, **2**, 279–286.
14 D. Petrović, B. Stojimirović, B. Petrović, Z. M. Bugarčić and Ž. D. Bugarčić, Studies of interactions between platinum(II) complexes and some biologically relevant molecules, *Bioorg. Med. Chem.*, 2007, **15**, 4203–4211.
15 C. Yu, K. H.-Y. Chan, K. M.-C. Wong and V. W.-W. Yam, Single-stranded nucleic acid-induced helical self-assembly of alkynylplatinum(II) terpyridyl complexes, *roc. Natl. Acad. Sci.*, 2006, **103**, 19652–19657.
16 S. D. Cummings, Platinum complexes of terpyridine: Interaction and reactivity with biomolecules, *Coord. Chem. Rev.*, 2009, **253**, 1495–1516.

17 P. J. Pages, D. L. Ang, E. P. Wright and J. R. Aldrich-Wright, Metal complex interactions with DNA, *Dalton Trans.*, 2015, **44**, 3505–3526.

18 K. Becker, C. Herold-Mende, J. J. Park, G. Lowe and R. H. Schirmer, Human thioredoxin reductase is efficiently inhibited by (2,2':6',2''-terpyridine)platinum(II) complexes. Possible implications for a novel antitumor strategy, *J. Med. Chem.*, 2001, **44**, 2784–2792.

19 G. Lowe, A. S. Droz, T. Vilaivan, G. W. Weaver, J. J. Park, J. M. Pratt, L. Tweedale and L. R. Kelland, Cytotoxicity of 2,2':6',2''-terpyridineplatinum(II) complexes against human ovarian carcinoma, *J. Med. Chem.*, 1999, **42**, 3167–3174.

20 R. J. Holmes, M. J. McKeage, V. Murray, W. A. Denny and W. D. McFadyen, cis-Dichloroplatinum(II) complexes tethered to 9-aminoacridine-4-carboxamides: synthesis and action in resistant cell lines in vitro, *J. Inorg. Biochem.*, 2001, **85**, 209–217.

21 B. E. Bowler, K. J. Ahmed, W. I. Sundquist, L. S. Hollis, E. E. Whang and S. J. Lippard, Synthesis, characterization, and DNA-binding properties of (1,2-diaminoethane) platinum(II) complexes linked to the DNA intercalator acridine orange by trimethylene and hexamethylene chains, *J. Am. Chem. Soc.*, 1989, **111**, 1299–1306.

22 Z. Ma, J. R. Choudhury, M. W. Wright, C. S. Day, G. Saluta, G. L. Kucera and U. Bierbach, A non-cross-linking platinum–acridine agent with potent activity in non-small-cell lung cancer, *J. Med. Chem.*, 2008, **51**, 7574–7580.

23 K. S. Al-Rashdi, B. A. Babgi, E. M. M. Ali, B. Davaasuren, A. Jedidi, A.-H. M. Emwas, M. A. Alrayyani, M. Jaremko, M. G. Humphrey and M. A. Hussien, Tuning Anticancer Properties of Pt(II) Complexes via Structurally Flexible N-(2-Picolyl)salicylimine Ligands, *RSC Adv.*, 2022, **12**, 27582–27595.

24 G. R. Fulmer, A. J. M. Miller, N. H. Sherden, H. E. Gottlieb, A. Nudelman, B. M. Stoltz, J. E. Bercaw and K. I. Goldberg, NMR chemical shifts of trace impurities: common laboratory solvents, organics, and gases in deuterated solvents relevant to the organometallic chemist, *Organometallics*, 2010, **29**, 2176–2179.

25 O. V. Dolomanov, L. J. Bourhis, R. J. Gildea, J. A. K. Howard and H. Puschmann, OLEX2: a complete structure solution, refinement and analysis program, *J. Appl. Crystallogr.*, 2009, **42**, 339–341.

26 G. M. Sheldrick, SHELXT - Integrated space-group and crystal-structure determination, *Acta Crystallogr.*, 2015, **A71**, 3–8.

27 G. M. Sheldrick, Crystal structure refinement with SHELXL, *Acta Crystallogr.*, 2015, **C71**, 3–8.

28 C. S. Devi, B. Thulasiram, S. Satyanarayana and P. Nagababu, Analytical techniques used to detect DNA binding modes of ruthenium(II) complexes with extended phenanthroline ring, *J. Fluoresc.*, 2017, **27**, 2119–2130.

29 W. Villarreal, L. Colina-Vegas, G. Visbal, O. Corona, R. S. Corrêa, J. Ellena, M. R. Cominetti, A. A. Batista and M. Navarro, Copper(I)–phosphine polypyridyl complexes: synthesis, characterization, DNA/HSA binding study, and antiproliferative activity, *Inorg. Chem.*, 2017, **56**, 3781–3793.

30 A. Erxleben, Investigation of non-covalent interactions of metal complexes with DNA in cell-free systems, *Chimia*, 2017, **71**, 102–111.

31 M. Lee, A. L. Rhodes, M. D. Wyatt, S. Forrow and J. A. Hartley, GC base sequence recognition by oligoimidazolecarboxamide and C-terminus-modified analogs of distamycin deduced from circular dichroism, proton nuclear magnetic resonance, and methidiumpropylethylenediaminetetraacetate-iron(II) footprinting studies, *Biochemistry*, 1993, **32**, 4237–4245.

32 D. P. Heller and C. L. Greenstock, Fluorescence lifetime analysis of DNA intercalated ethidium bromide and quenching by free dye, *Biophys. Chem.*, 1994, **50**, 305–312.

33 S. Alsaedi, B. A. Babgi, M. H. Abdellattif, M. N. Arshad, A.-H. M. Emwas, M. Jaremko, M. G. Humphrey, A. M. Asiri and M. A. Hussien, DNA-Binding and cytotoxicity of copper(I) complexes containing functionalized dipyridylphenazine ligands, *Pharmaceutics*, 2021, **13**, 764–777.

34 M. Amiri, K. Jankeje and J. R. Albani, Origin of Fluorescence Lifetimes in Human Serum Albumin. Studies on Native and Denatured Protein, *J. Fluoresc.*, 2010, **20**, 651–656.

35 S. Raut, R. Chib, S. Butler, J. Borejdo, Z. Gryczynski and I. Gryczynski, Evidence of energy transfer from tryptophan to BSA/HSA protected gold nanoclusters, *Methods Appl. Fluoresc.*, 2014, **2**, 035004.

36 H. Lineweaver and D. Burk, The Determination of Enzyme Dissociation Constants, *J. Am. Chem. Soc.*, 1934, **56**, 658–666.

37 A. S. Abdelhameed, A. H. Bakheit, F. M. Almutairi, H. AlRabiah and A. A. Kadi, Biophysical and In Silico Studies of the Interaction between the Anti-Viral Agents Acyclovir and Penciclovir, and Human Serum Albumin, *Molecules*, 2017, **22**, 1906.

38 B. A. Babgi, J. Alsayari, H. M. Alenezi, M. H. Abdellatif, N. E. Eltayeb, A.-H. M. Emwas, M. Jaremko and M. A. Hussien, Alteration of Anticancer and Protein-Binding Properties of Gold(I) Alkynyl by Phenolic Schiff Bases Moieties, *Pharmaceutics*, 2021, **13**, 461.

39 - M. J. Frisch, G. W. Trucks, H. B. Schlegel, G. E. Scuseria, M. A. Robb, J. R. Cheeseman, G. Scalmani, V. Barone, B. Mennucci and G. A. Petersson, *Gaussian 09. revision A.02*; Gaussian, Inc.: Wallingford, CT, USA, 2009.

40 - R. Dennington, R. T. Keith, J. Millam and V. Gauss, *Version 5, vol Shawnee Mission*, Semichem, Inc., 2009.

41 P. J. Stephens, F. J. Devlin, C. F. Chabalowski and M. J. Frisch, Ab initio calculation of vibrational absorption and circular dichromism spectra using density functional force fields, *J. Phys. Chem.*, 1994, **98**, 11623–11627.

42 D. Moran, A. C. Simmonett, F. E. Leach III, W. D. Allen, P. v. R. Schleyer and H. F. Schaefer, Popular theoretical methods predict benzene and arenes to be nonplanar, *J. Am. Chem. Soc.*, 2006, **128**, 9342–9343.

43 M. Dolg, H. Stoll and H. Preuss, Energy-adjusted *ab initio* pseudopotentials for the rare earth elements, *J. Chem. Phys.*, 1989, **90**, 1730–1734.

44 S. Grimme, J. Antony, S. Ehrlich and H. Krieg, A consistent and accurate *ab initio* parametrization of density

functional dispersion correction (DFT-D) for the 94 elements H-Pu, *J. Chem. Phys.*, 2010, **132**, 154104.

45 - E. D. Glendenning, A. E. Reed, J. E. Carpenter and F. Weinhold, *NBO; version 3.1*, Gaussian Inc., Pittsburg, PA, USA, 2001.

46 E. M. Ali, A. A. Elashkar, H. Y. El-Kassas and E. I. Salim, Methotrexate loaded on magnetite iron nanoparticles coated with chitosan: Biosynthesis, characterization, and impact on human breast cancer MCF-7 cell line, *Int. J. Biol. Macromol.*, 2018, **120**, 1170–1180.

47 J. A. Plumb Cell sensitivity assays: the MTT assay, in *Cancer cell culture*, Springer, 2004, pp. 165–169.

48 J. Fried, A. G. Perez and B. D. Clarkson, Flow cytofluorometric analysis of cell cycle distributions using propidium iodide. Properties of the method and mathematical analysis of the data, *J. Cell Biol.*, 1976, **71**, 172–181.

49 K. W. Jennette, S. J. Lippard, G. A. Vassiliades and W. R. Baueri, Metallointercalation Reagents. 2-Hydroxyethanethiolato(2,2',2"-terpyridine)-platinum(I1) Monocation Binds Strongly to DNA By Intercalation, *Proc. Natl. Acad. Sci. U. S. A.*, 1974, **71**, 3839–3843.

50 M. Howe-Grant, K. C. Wu, W. R. Bauer and S. J. Lippard, Binding of Platinum and Palladium Metallointercalation Reagents and Antitumor Drugs to Closed and Open DNAs, *Biochemistry*, 1976, **15**, 4339–4346.

51 P. J. Bond, R. Langridge, K. W. Jennette and S. J. Lippard, X-ray fiber diffraction evidence for neighbor exclusion binding of a platinum metallointercalation reagent to DNA, *Proc. Natl. Acad. Sci. U. S. A.*, 1975, **72**, 4825–4829.

52 F. J. Meyer-Almes and D. Porschke, Mechanism of intercalation into the DNA double helix by ethidium, *Biochemistry*, 1993, **32**, 4246–4253.

53 W. R. Ware, Oxygen quenching of fluorescence in solution: An experimental study of the diffusion process, *J. Phys. Chem.*, 1962, **66**, 455–458.

54 Z. Seferoğlu, M. M. A. Mahmoud and H. Ihmels, Studies of the binding interactions of dicationic styrylimidazo[1,2-a] pyridinium dyes with duplex and quadruplex DNA, *Dyes Pigm.*, 2016, **125**, 241–248.

55 N. Busto, M. Martínez-Alonso, J. M. Leal, A. M. Rodríguez, F. Domínguez, M. I. Acuña, G. Espino and B. García, Monomer–dimer divergent behavior toward DNA in a half-sandwich ruthenium(II) aqua complex. Antiproliferative biphasic activity, *Organometallics*, 2015, **34**, 319–327.

56 J. A. Platts, M. Ravera, E. Gabano, M. Sardi, S. Bianco and D. Osella, Solvolysis of a series of cisplatin-like complexes – Comparison between DNA-biosensor and conductivity data, *Eur. J. Inorg. Chem.*, 2012, 5625–5631.

57 T. Lazarevic, A. Rilak and Z. D. Bugarcic, Platinum, palladium, gold and ruthenium complexes as anticancer agents: Current clinical uses, cytotoxicity studies and future perspectives, *Eur. J. Med. Chem.*, 2017, **142**, 8–31.

58 D. Gibellini, F. Vitone, P. Schiavone, C. Ponti, M. La Placa and M. C. Re, Quantitative detection of human immunodeficiency virus type 1 (HIV-1) proviral DNA in peripheral blood mononuclear cells by SYBR green real-time PCR technique, *J. Clin. Virol.*, 2004, **29**, 282–289.

59 J. R. Lakowicz, *Principles of Fluorescence Spectroscopy*, Springer, New York, NY, USA, 3rd edn, 2006.

60 G. Vignesh, S. Arunachalam, S. Vignesh and R. A. James, BSA binding and antimicrobial studies of branched polyethyleneimine–copper(II)bipyridine/phenanthroline complexes, *Spectrochim. Acta, Part A*, 2012, **96**, 108–116.

61 E. Lissi, C. Calderón and A. Campos, Evaluation of the Number of Binding Sites in Proteins from their Intrinsic Fluorescence: Limitations and Pitfalls, *Photochem. Photobiol.*, 2013, **89**, 1413–1416.

62 S. Alsaedi, B. A. Babgi, M. H. Abdellatif, A.-H. Emwas, M. Jaremko, M. G. Humphrey and M. A. Hussien, Effect of Net Charge on DNA-Binding, Protein-Binding and Anticancer Properties of Copper(I) Phosphine-Diimine Complexes, *J. Inorg. Organomet. Polym.*, 2021, **31**, 3943–3952.

63 S. Tanida, T. Mizoshita, K. Ozeki, H. Tsukamoto, T. Kamiya, H. Kataoka, D. Sakamuro and T. Joh, Mechanisms of cisplatin-induced apoptosis and of cisplatin sensitivity: potential of BIN1 to act as a potent predictor of cisplatin sensitivity in gastric cancer treatment, *Int. J. Surg. Oncol.*, 2012, **2012**, 862–879.